

# How to Evaluate Medical Visualizations on the Example of 3D Aneurysm Surfaces

S. Glaßer<sup>1</sup>, P. Saalfeld<sup>1</sup>, P. Berg<sup>2</sup>, N. Merten<sup>1</sup>, B. Preim<sup>1</sup>

<sup>1</sup> Department for Simulation and Graphics, Otto-von-Guericke University Magdeburg, Germany

<sup>2</sup> Department of Fluid Dynamics and Technical Flows, Otto-von-Guericke University Magdeburg, Germany

---

## Abstract

*For the evaluation of medical visualizations, a ground truth is often missing. Therefore, the evaluation of medical visualizations is often restricted to qualitative comparisons w.r.t user preferences but neglects more objective measures such as accuracies or task completion times. In this work, we provide a pipeline with statistical tests for the evaluation of the user performance within an experimental setup. We demonstrate the adaption of the pipeline for the specific example of cerebral aneurysm surface visualization. Therefore, we developed three visualization techniques to compare the aneurysm volumes. Then, we present a single-factor, within-subject user study, which allows for the evaluation of these visualization techniques as well as the identification of the most suitable one. The evaluation includes a qualitative as well as a comprehensive quantitative analysis to determine statistically significant differences. As a result, a color-coded map surface view is identified as best suited to depict the aneurysm volume changes. The presentation of the different stages of the evaluation pipeline allows for an easy adaption to other application areas of medical visualization. As a result, we provide orientation to enrich qualitative evaluations by the presented quantitative analyses.*

Categories and Subject Descriptors (according to ACM CCS): I.3.3 [Computer Graphics]: Picture/Image Generation—Line and curve generation G.3 Probability and Statistics Experimental Design

---

## 1. Introduction

Nowadays, many approaches for supporting the clinical expert as well as the clinical researcher regarding diagnosis or therapy involve a number of computer-supported segmentation, visualization and evaluation steps. In this paper, we explain how to evaluate comparative medical visualizations. Although many authors conduct a qualitative evaluation with medical domain experts, those results are hardly reproducible. Often, these domain experts are cooperation partners and co-authors of the presented work, where a subjective bias is hardly avoidable. Nevertheless, their medical knowledge is essential for specific application areas which may justify this procedure. Therefore, we do not neglect qualitative studies, but we want to include quantitative statistical analyses such that they can be easily adapted by other medical visualization researchers for a more comprehensive evaluation.

The segmentation of vessels with pathologic changes such as aneurysms or stenoses is an important research area. To create reproducible results as well as to reduce the work load of clinicians, automatic segmentations of vascular structures are desired. Due to patient-specific anatomies and pathologies, such automatic solutions remain challenging, and aiming for a general automatic segmentation framework is probably illusory [LABFL09]. Our application area is the visualization of cerebral aneurysms. Aneurysms

bear the risk of rupture, which may cause severe consequences for the patients. For an improved intervention planning, patient-specific 3D surface models of the aneurysm and the surrounding vascular tree are extracted. They allow for the simulation of the internal blood flow [CCA\*05, BRB\*15] or the extraction of morphological parameters [LEBB09]. The results are included into the minimally invasive surgical plan as well as the post-processing applications within the clinical environment.

Our application scenario does not focus on the segmentation technique, but rather on the comparative visualization of different segmentation results. The employed surface meshes were extracted with a threshold-based segmentation, which can be successfully used for cerebral aneurysms [GBNP15]. However, during the segmentation process, the clinical expert requires feedback how parameters influence the segmentation results since small parameter changes may induce enormous changes of the surface mesh. To guide the clinical expert through the segmentation process, we developed three different comparative visualization techniques to show surface mesh variations.

Our quantitative and qualitative evaluation allows for the identification of the most suitable visualization technique. It comprises the visualization of five cerebral aneurysms, each approximated with three slightly different surface meshes. Our conducted user

study determines which visualization technique is best suited to evaluate the perception of small changes in the aneurysm volumes. This is especially necessary when the clinical expert or medical researcher tunes the parameters of the segmentation process and requires feedback, whether the aneurysm extent increases or not. The presented concepts comprising the experimental setup, the study design, the study procedure as well as the statistical evaluation, can be easily generalized and thus, transferred to other medical visualization application areas. Our contributions are:

- We explain which statistical test is suitable for analysis of a user study and order them into a general pipeline for the qualitative and quantitative evaluation of medical visualizations.
- We use the application scenario of cerebral aneurysms to provide three techniques  $Vis_A$ ,  $Vis_B$ , and  $Vis_C$  for the visualization of two similar but not identical aneurysm surface meshes, which mutually penetrate and overlap.
- Based on this example, we demonstrate how to employ the pipeline to determine which visualization technique is best suited for this application.

## 2. Related Work

In this section, we discuss related work for the qualitative and quantitative evaluation of visualizations with focus on the application area of aneurysms and vessels. We also refer to comparative visualizations of surface meshes extracted from medical image data.

In recent years, findings from psychophysical studies were incorporated to enhance 2D and 3D visualizations [BCFW08] influencing also the evaluation process of visualizations. For the assessment of a visualization's suitability and performance, user studies offer a scientifically sound method [KHI\*03]. Isenberg et al. [IIC\*13] provide a systematic review of the evaluation practices in visualization. They employ several evaluation categories and conclude that the *Qualitative Result Inspection* was most often used by all reviewed papers. Further emphasis on evaluation of algorithmic performance as well as an increasing trend in the evaluation for user experience and user performance were reported.

This finding is also reflected in medical visualizations. Often, a user study is carried out, where the participants provide a subjective rating of the novel algorithm. Gasteiger et al. [GNKP10] carried out a user study for their aneurysm visualization based on the participant's grade of satisfaction w.r.t. depth perception, spatial relationships, flow perception and surface shape. Subsequently, a more quantitative evaluation was presented by Baer et al. [BGCP11] for this visualization technique amongst two others. They conducted three controlled, task-based experiments and were able to determine statistically significant differences for the visualizations. Borkin et al. [BGP\*11] also includes a formal quantitative user study to determine which visualization technique of the endothelial shear stress of coronary arteries is best suited. Hence, the experimental study provided by Díaz et al. [DRN\*15] comprises a test setup to evaluate different shading techniques for volume data sets. Their evaluation included a quantitative statistical analysis as well. Also, perceptually motivated medical visualizations often include quantitative evaluations [PBC\*16]. However, they focus on abstract information, e.g., depth perception, rather than comparing visualization techniques for a specific medical application area.

Visualizations of vessels are often depicted as 3D surfaces due to their complex and patient-individual shape [BFLC04, SOBP07, PO08]. Furthermore, overview visualizations are possible, e.g., the CoWRadar visualization for cerebral vessels [MMNG15]. Since we intend to employ aneurysm surface meshes for subsequent computational fluid dynamics (CFD) simulations and morphological analyses, we focus on 3D surface visualization methods. The depiction of cerebral aneurysms mostly involves the visual representation of hemodynamic parameters, e.g., scalar parameters are displayed via color-coded surface views [CSP10]. Gasteiger et al. [GNKP10] developed an illustrative visualization of aneurysms using a Fresnel shading to reveal the embedded blood flow. This work strongly motivated our visualization technique  $Vis_B$ .

Our comparative visualization is inspired by the image-based rendering of intersecting surfaces [BBF\*11]. This technique is based on the approach by Weigle and Taylor [WT05]. Next to the integration of additional local distance cues, they enabled interactive manipulation of the surfaces. Geurts et al. [GSK\*15] employed a visual comparison of medical segmentation results to allow for an evaluation of the segmentation quality. They provided additional information with landmark-based clustering to detect similar segmentation results. For the visualization itself, a color-coding of the surface was employed. There also exist illustrative approaches, e.g., the visualization presented by Carnecky et al. [CFM\*13]. However, we aim at a fast comparison of cerebral aneurysm volume. Therefore, we want to reduce the visual complexity and choose the concepts provided by Busking et al. [BBF\*11] as inspiration for our technique  $Vis_C$ .

Our visualization techniques show different segmentation results from the same patient which can be also interpreted as uncertainty visualization. Grigoryan and Rheingans [GR04] presented point-based probabilistic surfaces, which visualize surface models of medical structures such as tumors. Hence, the surface points are displaced to reflect the uncertainty at that point. The method by Pöthkow and Hege [PH11] comprises a feature-based visualization for isosurfaces with uncertainties. Their approach employs color-coding, glyphs and direct volume rendering. A taxonomy of uncertainty visualization approaches is provided by Potter et al. [PRJ12].

## 3. Medical Background and Image Data

Cerebral aneurysms are pathologic dilatations of the cerebral artery walls which may rupture and cause a subarachnoid hemorrhage with severe consequences for the patient. Treatment is carried out via endovascular intervention or neurosurgical clipping. However, the treatment itself may cause complications such as hemorrhages. The mortality rate associated with treatment is reported to be higher than the rupture rate of small asymptotic aneurysms [Wie03]. Thus, rupture risk assessment is an active clinical research area.

Rupture risk factors in clinical practice mainly comprise the aneurysm's morphology as well as the type of aneurysm, i.e., asymptomatic or symptomatic [WvdSAR07]. Hence, extraction of surface meshes for aneurysms provide additional information such as the evaluation of the ostium area (i.e., the orifice between the aneurysm sac and the parent artery) [LEBB09]. Further research directions involve the simulation of the internal blood flow since

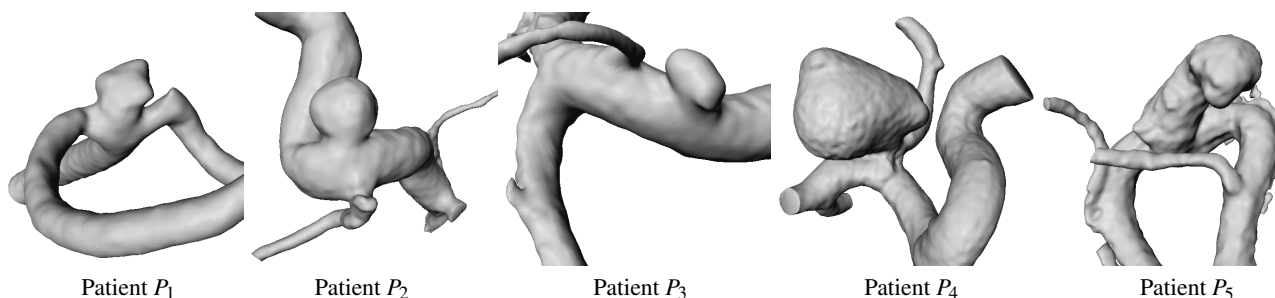


**Figure 1:** Surface meshes of five patient data sets  $P_1$ - $P_5$  reconstructed with the HU normal kernel are shown.

unstable and complex blood flow was correlated with increased rupture risk [CCA\*05, XNT\*11]. Again, a patient-specific surface mesh is the prerequisite for volume grid extraction and a subsequently CFD simulation.

For diagnosis of cerebral aneurysms, rotational angiography (RA) is considered as gold standard imaging method [GLR\*09] due to the high spatial resolution. Based on RA data, the 3D digital subtraction angiography (DSA) data sets are reconstructed. To obtain the slightly similar surface meshes, we exploit the reconstruction process of the RA data from the DSA suite (Siemens Artis zeego, Siemens Healthcare GmbH, Erlangen, Germany). Five patient-specific cerebral aneurysm data sets ( $D_1$ - $D_5$ ) were reconstructed using three different kernels: Hounsfield unit (HU) smooth, HU normal and HU sharp. The five aneurysms stem from five female patients with mean age of 49 years (range 45-59 years). One cerebral aneurysm was located at the anterior communicating artery, one at the posterior communicating artery, two at the segment of the internal carotid artery, and one at the bifurcation of the middle cerebral artery. Their size varied from 2.5 mm to 11.2 mm. All patients were treated with endovascular coiling.

#### 4. Segmentation and Comparative Visualization of Cerebral Aneurysms

In this section, the aneurysm and ostium segmentation is explained. Afterwards, the three visualization techniques  $Vis_A$ ,  $Vis_B$  and  $Vis_C$  are presented.

##### 4.1. Segmentation of Aneurysm and Ostium

For each patient's RA data set, the three different reconstruction kernels yield three different DSA data sets. For each patient, a threshold-based segmentation was carried out for the HU normal reconstructed DSA image data. The resulting surface meshes are depicted in Figure 1. Next, the remaining reconstructions of the same patient were carried out such that they exhibit similar contours in a representative slice covering the aneurysm (see Fig. 2). Based on each threshold, the iso-surface is extracted and converted into the triangle surface mesh. Data inspection, threshold segmentation and mesh generation was carried out in MeVisLab 2.7 (MeVis Medical Solutions AG, Bremen, Germany). Hence, the segmentation was not the focus of our work and depending on the medical application, a fully automatic segmentation can be employed

as well. For the purpose of our study, we required similar, but not identical aneurysm surface meshes, which could be successfully extracted with the threshold-based segmentation from different reconstructed RA data sets.

Our visualizations focus on the comparison of the volume of each aneurysm without the surrounding vessel tree. Therefore, visual separation between aneurysm and parent vessel has to be provided. The ostium was manually extracted by defining a closed cutting line along the aneurysm surface mesh using Blender 2.74 (Blender Foundation, Amsterdam, The Netherlands). This cutting line was employed twice. First, we create a closed ostium surface by triangulating the cutting line. The aneurysm surface was cut with this surface to extract the aneurysm's volume for our evaluation. Second, the cutting line's vertices were extruded to create a ruff-like structure, which supports the participants of our user study. An automatic ostium segmentation was not the focus of this paper, but interested readers are referred to Neugebauer et al. [NLBP13].

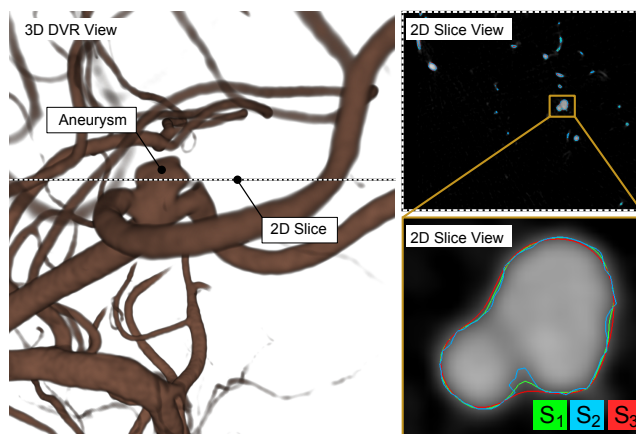


**Figure 2:** Segmentations of patient  $P_1$ . On the left, a direct volume rendering of the DSA data set is depicted. A 2D slice covering the aneurysm is shown on the right, its position is also highlighted in the 3D view. Thresholds for segmentations  $S_1$ - $S_3$  are selected such that similar segmentations are achieved, see bottom right. The resulting segmentation masks are color-coded.

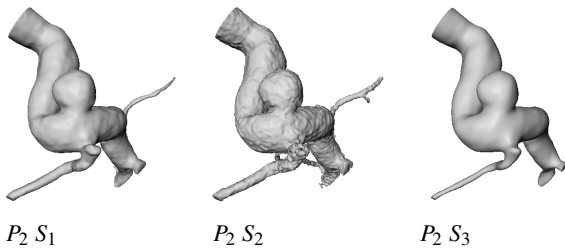


**Figure 3:** For patient  $P_2$ , the three resulting segmentations  $S_1$ ,  $S_2$  and  $S_3$  based on the different reconstruction kernels (HU normal, HU sharp, HU smooth) are depicted.

## 4.2. Comparative Visualization Techniques

To evaluate differences of the aneurysm volume, we developed three visualization techniques: the iso-surface view  $Vis_A$ , the boundary-enhancing shading view  $Vis_B$ , and the color-coded map surface view  $Vis_C$ . Each technique shows two aneurysms, where the first one is referred to as  $A_{Ref}$ , i.e., the reference aneurysm, and the second one as  $A_{Comp}$ , i.e., the aneurysm for comparison. Note that the ordering of the aneurysms is important, and employing  $A_{Ref}$  first and  $A_{Comp}$  second yields a different visualization result than the usage of  $A_{Comp}$  first and  $A_{Ref}$  second. In the following, the visualization techniques will be described in more detail.

### 4.2.1. The Iso-Surface View - $Vis_A$

The iso-surface view is a rather straightforward direct visualization of the two surface meshes of the aneurysms  $A_{Ref}$  and  $A_{Comp}$ . It is realized in MeVisLab using the Open Inventor Library. For  $A_{Ref}$  an orange, and for  $A_{Comp}$  a cyan transparent surface mesh is simultaneously visualized with opacity values of 0.5 (see Fig. 4). Beyond mesh extraction, no further preprocessing is required.

### 4.2.2. The Boundary-Enhanced View - $Vis_B$

The second visualization technique  $Vis_B$  (see Fig. 5) is based on the Fresnel shading approach, which was successfully employed for aneurysm visualization comprising an inner blood flow visualization [GNKP10] or the outer vessel wall revealing the color-coded inner vessel wall [GLH\*14]. This technique is also referred to as ghosted view or x-ray shading. Although we do not include additional information yet, e.g., the inner blood flow, we do integrate this visualization technique in our user study since we are interested in a possible extension of the visualization with the above-mentioned information in the future.

The opacity  $o$  for each surface mesh is assigned in the fragment shader and depends on the normal  $n$  and the viewing vector  $v$ :

$$o = 1 - (\vec{n} \cdot \vec{v})^f,$$

where  $f$  serves as edge-fall-off parameter. This parameter strongly influences the visualization of possible inner structures. We use an empirically determined value of  $f = 0.7$ . The visualization technique is realized in MeVisLab using the Open Inventor vertex and fragment shader modules, where the user can directly provide shader codes as input.

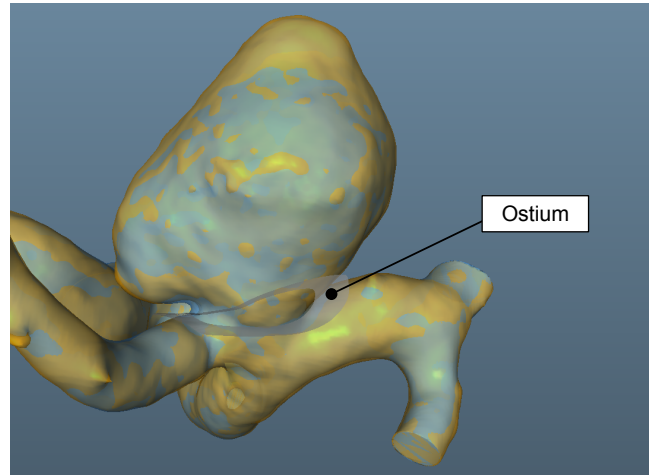


**Figure 4:** Depiction of the iso-surface view  $Vis_A$ . In case the surface mesh of  $A_{Ref}$  exceeds the surface mesh of  $A_{Comp}$ , the orange surface becomes visible. Otherwise, the cyan mesh is visible. The ruff-like structure provides information about the ostium.

### 4.2.3. Map-Surface-View - $Vis_C$

In contrast to  $Vis_A$  and  $Vis_B$ , the map surface view visually provides quantitative information for the distance between  $A_{Ref}$  and  $A_{Comp}$ . For the gathering of the distance information, the estimation of the nearest vertex pairs from  $A_{Ref}$  and  $A_{Comp}$  is carried out. We calculate the normals of the  $A_{Ref}$  surface mesh and approximate the distance based on the intersection with  $A_{Comp}$ . The normals of  $A_{Ref}$  point inwards. If  $A_{Comp}$  is larger than  $A_{Ref}$ , the intersection in negative normal direction is nearer to  $A_{Ref}$ 's vertex than the intersection in positive normal direction and the distance value is stored as negative value.

For visual representation, we transfer the extracted distance values to the interval  $[0, 1]$  since we want to store them as texture coordinates. Therefore, we clamp the original distance values to the interval  $[-0.1, 0.1]$  mm and rescale them to  $[0, 1]$ . Thus, texture values of 0.5 are assigned to parts where the surface meshes of  $A_{Ref}$  and  $A_{Comp}$  have a distance of almost 0 mm. Finally, we employ the color map depicted in Figure 6 as texture and obtain  $Vis_C$  by using the Open Inventor Vertex Attributes module provided in MeVisLab. The color map is designed such that areas where  $A_{Ref}$  is larger than  $A_{Comp}$  are mapped to orange, whereas the quantitative distance information is provided by the hue's saturation. Blue areas indicate a larger local extent of  $A_{Comp}$ .

## 5. Comparative Study

In this section, we present our pipeline for a qualitative and quantitative evaluation. Afterwards, we describe our experimental setup and the user study in more detail.

### 5.1. A Pipeline for the Evaluation of Medical Visualizations

Based on the studies presented and discussed in Section 2, as well as discussions with statistical researchers, we created a generaliz-



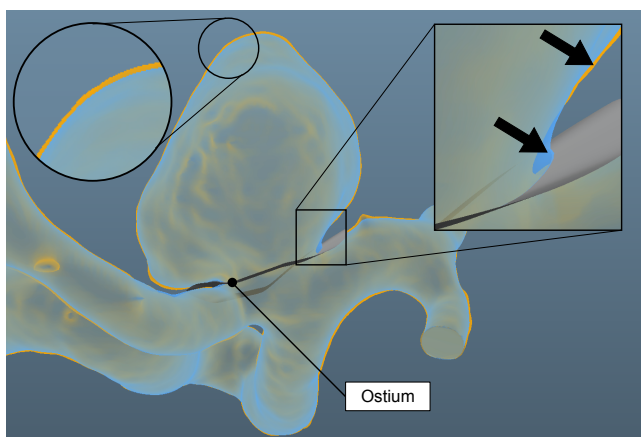


**Figure 5:** Depiction of  $Vis_B$ . The mesh extents become best visible at the boundary of the aneurysm (see circular inlay), which requires an interactive exploration of the 3D scene. The visualization shows a larger volume of  $A_{ref}$  at the aneurysm itself, but not at the aneurysm neck (see rectangular inlay and arrows).

able pipeline, see Figure 7. The pipeline is reduced to the scenario of a single-factor study with one independent variable. For our application, the independent variable is the visualization with levels  $Vis_A$ ,  $Vis_B$  and  $Vis_C$ . For generalization, the independent variable is provided by the medical visualization.

First, the researcher decides whether to carry out a qualitative analysis, e.g., the participants attitude towards a technique, or a quantitative analysis, e.g., to provide statistically significant results, or both. Second, user performance tasks have to be defined. Most often accuracy, e.g., the number of correct answers, and task completion time are chosen. Also the study type, i.e. between-subject design (aiming at differences between the participants) or within-subject design (aiming at the variability of a particular value for individuals in a sample), has to be chosen, which depends on the available participants. Advantageously, between-subject studies avoid learning effects and the evaluation time is reduced for each participant compared to within-subject studies. However, groups of similar participants (w.r.t. age, experience, knowledge, etc.) have to be recruited. Especially in the medical domain, these prerequisites are not easily met. On the other side, within-subject studies avoid interpersonal differences. However, they may suffer from learning or sequence effects and intrapersonal differences.

After acquiring the user performances, a test is carried out to check for a normal distribution. We can use the Shapiro-Wilk test for this purpose. This stage is a prerequisite to choose the appropriate test in the next step. We analyze whether there is a significant difference between the levels of our independent variable via an *analysis of variance* (ANOVA). If we can assume normal distribution, i.e., the data is parametric, a one-way ANOVA (due to our single-factor study) is carried out. Otherwise, we employ the Friedmann test for the non-parametric data. If there is a significant difference between the metrics, we can examine this difference in more detail with a pairwise comparison. For example, a pair-wise comparison of the non-parametric test result for a within-subject

study can be carried out with the Wilcoxon signed rank test. If no significant differences exist, we also obtained an important information. We can furthermore provide descriptive results such as the mean  $\mu$ , the median  $m$  or the standard deviation  $\sigma$  to compare the results. Hence, interpretation of  $\sigma$  should take the data's distribution into account. In addition, a box plot visualization provides an important overview including information about the distribution.

Based on the infinite configuration of user studies, this pipeline is presented with no claim to completeness. However, it can be easily generalized to various application scenarios, i.e., after determining the user performance, a check for normal distribution is carried out. Next, a check for significant differences (based on one or more independent variables) and a subsequently pairwise comparison (based on one or more independent variables and within- and between-subject study design) is applied.

## 5.2. Experimental Setup

The whole study was realized with MeVisLab. Thus, each participant was presented with a graphical user interface (GUI), which guided the participants through the study. The user interface was created with a TabView object using hidden tabs. Each time the participant answered a question via clicking a button, the next tab was shown. At first, the TabView comprises slides for medical background information. Since all visualization techniques were implemented in MeVisLab, they could be easily integrated in the TabView GUI as well. Selection of visualization techniques and data sets for the participants was automatically carried out via Python scripts. Also, the logging of user inputs and time required for each task, i.e., the task completion time, were stored as text files.

## 5.3. Study Design

For the comparison of the 3D visualizations, we design a single-factor and within-subject study. The independent variable (i.e., the

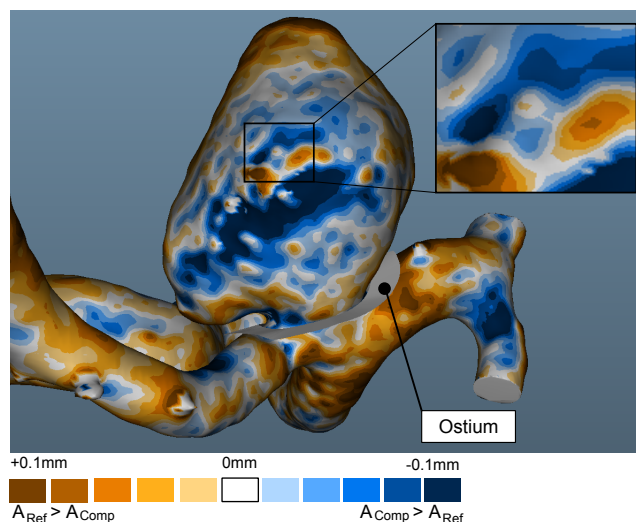


**Figure 6:** Depiction of visualization  $Vis_C$ . The inlay highlights the aneurysm surface.

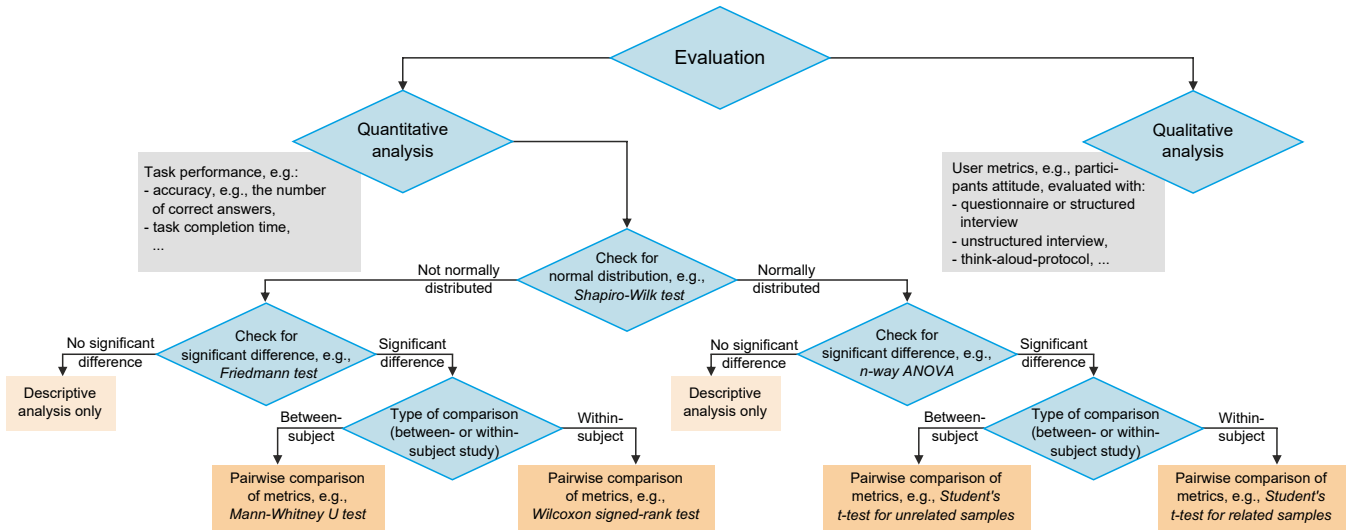


Figure 7: The proposed pipeline represented as decision tree for the qualitative and quantitative evaluation.

single factor) is the visualization technique which has three levels:  $Vis_A$ ,  $Vis_B$  and  $Vis_C$ . The two dependent variables for each visualization are the task completion time and accuracy. Accuracy is defined as the number of correct answers, i.e., the number of right decisions whether aneurysm  $A_{Ref}$  or  $A_{Comp}$  is larger. Each experiment is carried out via a within-subject design such that each participant is confronted with each visualization technique six times. Thus, the amount of different visualization techniques shown is balanced.

Basically, we repeat the same question whether  $A_{Ref}$  is larger than  $A_{Comp}$  18 times. To reduce the influence of confounder variables, e.g., training or sequence effects, we change the order of the shown visualization techniques as well as the employed patient and segmentation data with *a-priori pseudo randomization*. The pseudo randomization is listed in detail in Tab. 1, Tab. 2 and Tab. 3. For example, for the first test  $T_1$  and the first question  $q_1$ , the user is provided with  $Vis_A$  of the data sets from patient  $P_1$ , whereas  $S_1$  is employed for the reference aneurysm  $A_{Ref}$  and  $S_2$  for the comparison aneurysm  $A_{Comp}$ . In general, for the  $i$ -th test  $T_i$  with questions  $q_1$ - $q_{18}$ , each visualization  $Vis_A$ ,  $Vis_B$ , and  $Vis_C$  was shown six times in the pseudo-randomized order. The patient data  $P_1 - P_5$  was alternated (see Tab. 2) as well as the segmentations (see Tab. 3). Since the order of the shown data sets was important, each test is repeated for switched segmentation combinations, i.e.,  $T_1$  is identical to  $T_2$  w.r.t. visualization technique and patient but not segmentation.

The pseudo-randomization ensures that each user evaluates different data sets with varying segmentations, i.e., the user does not see the same visualization technique with the same data sets for  $A_{Ref}$  and  $A_{Comp}$  twice. This also holds for the demonstration of visualizations during the introduction (see Sec. 5.4), where the combinations of patient data and visualization techniques were not identical to the ones used in the test.

Next to the users' choices regarding the aneurysm volumes, we logged the task completion time as well as the answers to the following questionnaire:

- the age,
- the sex,
- whether the user is familiar with 3D visualizations,
- whether the user is familiar with 3D medical image data,
- a rating for  $Vis_A$ ,  $Vis_B$  and  $Vis_C$  whether the technique was suitable to analyze which aneurysm was larger, and
- a rating for  $Vis_A$ ,  $Vis_B$  and  $Vis_C$  how much the user liked it.

The ratings were assessed with a 5-point Likert scale ranging from -- (i.e. not suitable at all or not preferable at all) to ++ (i.e. very suitable or very preferable).

Table 1: Pseudo-randomization for the visualizations. For the test  $T_i$  with questions  $q_1$ - $q_{18}$ ,  $Vis_A$ ,  $Vis_B$ , and  $Vis_C$  were shown six times in the depicted order. Each test is repeated for switched segmentation combinations. After  $T_{12}$ , the sequence is repeated.

	$q_1$ - $q_6$	$q_7$ - $q_{12}$	$q_{13}$ - $q_{18}$
$T_1$	$Vis_A$	$Vis_B$	$Vis_C$
$T_2$	$Vis_A$	$Vis_B$	$Vis_C$
$T_3$	$Vis_A$	$Vis_C$	$Vis_B$
...	...	...	...
$T_5$	$Vis_B$	$Vis_A$	$Vis_C$
...	...	...	...
$T_7$	$Vis_B$	$Vis_C$	$Vis_A$
...	...	...	...
$T_9$	$Vis_C$	$Vis_A$	$Vis_B$
...	...	...	...
$T_{11}$	$Vis_C$	$Vis_B$	$Vis_A$
...	...	...	...
$T_{13}$	$Vis_A$	$Vis_B$	$Vis_C$
...	...	...	...

**Table 2:** Pseudo-randomization for the patient data. For the test  $T_i$  with questions  $q_1$ - $q_{18}$ , the patient data  $P_1 - P_5$  was alternated, starting with  $P_1$  for  $q_1 - q_3$  and the segmentations  $S_1$ - $S_2$ ,  $S_2$ - $S_3$ ,  $S_3$ - $S_1$  (see Tab. 3). The ordering of patients is repeated after  $T_{10}$ .

	$q_1$ - $q_3$	$q_4$ - $q_6$	$q_7$ - $q_9$	$q_{10}$ - $q_{12}$	$q_{13}$ - $q_{15}$	$q_{16}$ - $q_{18}$
$t_1$	$P_1$	$P_2$	$P_3$	$P_4$	$P_5$	$P_1$
$t_2$	$P_1$	$P_2$	$P_3$	$P_4$	$P_5$	$P_1$
$t_3$	$P_2$	$P_3$	$P_4$	$P_5$	$P_1$	$P_2$
...	...	...	...	...	...	...
$t_5$	$P_3$	$P_4$	$P_5$	$P_1$	$P_2$	$P_3$
...	...	...	...	...	...	...
$t_7$	$P_4$	$P_5$	$P_1$	$P_2$	$P_3$	$P_4$
...	...	...	...	...	...	...
$t_9$	$P_5$	$P_1$	$P_2$	$P_3$	$P_4$	$P_5$
...	...	...	...	...	...	...
$t_{11}$	$P_1$	$P_2$	$P_3$	$P_4$	$P_5$	$P_1$
...	...	...	...	...	...	...

**5.4. Procedure**

The GUI was presented to each participant, starting with a slide for the medical background information. Afterwards, the three different visualizations  $Vis_A$ ,  $Vis_B$ , and  $Vis_C$  were shown. Each of the visualizations as well as the interaction, e.g., zooming and rotating, was explained in detail by the supervisor. The user was also encouraged to explore the scene and get familiar with the user interface for 3D exploration provided by MeVisLab. The test number  $t_i$  was assigned to the  $i$ -th user. The user had to answer 18 questions  $q_1$ - $q_{18}$  and decide, which aneurysm possess the larger volume. Finally, the users answered the questionnaire.

**6. Results**

This section describes the participants and lists the results of the user study including quantitative and descriptive analyses, based on our evaluation pipeline (recall Fig. 7). Afterwards, the qualitative subjective ratings w.r.t. suitability and preferability are discussed.

**6.1. Participants**

The participants were recruited from visitors of the *Long Night of Sciences*. During this event, scientific institutes show experiments

**Table 3:** Pseudo-randomization for the segmentations. For the test  $T_i$  with questions  $q_1$ - $q_{18}$  two different segmentations of the same patient were employed. For example,  $S_1$ - $S_2$  indicates segmentation  $S_1$  for  $A_{Ref}$  and segmentation  $S_2$  for  $A_{Comp}$ . Since the order of the shown data sets was important, the order of segmentations is reversed for odd tests.

	$q_{1,4,7,10,13,16}$	$q_{2,5,8,11,14,17}$	$q_{3,6,9,12,15,18}$
$T_1$	$S_1$ - $S_2$	$S_2$ - $S_3$	$S_3$ - $S_1$
$T_2$	$S_2$ - $S_1$	$S_3$ - $S_2$	$S_1$ - $S_3$
$T_3$	$S_1$ - $S_2$	$S_2$ - $S_3$	$S_3$ - $S_1$
...	...	...	...

**Table 4:** Data from the user study. For each user  $U_1$ - $U_{34}$ , the number of correct answers for  $Vis_A$ ,  $Vis_B$  and  $Vis_C$  is extracted. This value ranges from 0 to 6, since each participant was confronted with each technique six times. Also, for each user the average time  $t_A$ ,  $t_B$  and  $t_C$  (provided in seconds) to answer a question is collected.

	Correct answers			Average required time		
	$Vis_A$	$Vis_B$	$Vis_C$	$t_A$	$t_B$	$t_C$
$U_1$	5	2	5	22 s	20.17 s	17.67 s
...	...	...	...	...	...	...
$U_{34}$	5	4	5	17.83 s	10.67 s	15.33 s

and tests to the general public. The majority of our participants were from the university’s computer science and medical engineering departments. As a result, we were able to conduct a user study with 34 participants comprising 5 female and 29 male users, aging from 16 - 66 years. When asked if the users have experiences with medical visualizations, 10 users declined and 24 affirmed. Regarding the experience with 3D visualizations, eight users stated they have no experience. We did not include domain experts or prospective users since we were only interested in a perceptual evaluation of volume change. Hence, no medical knowledge was required.

**6.2. Evaluation**

The data collection provided by the conducted user study is listed in Table 4. The participants’ answers form the set of observations for  $Vis_A$ ,  $Vis_B$  and  $Vis_C$ . We also collect the set of averaged task completion times  $t_A$ ,  $t_B$ , and  $t_C$ , each participant needed for  $Vis_A$ ,  $Vis_B$  and  $Vis_C$ . All statistical tests were carried out with SPSS 22.0 (IBM, New York, USA). Our statistical analysis comprises three stages (recall Fig. 7):

1. We determine whether there is a significant difference between the visualizations w.r.t. accuracy.
2. In case the visualizations are significantly different, we further analyze which visualization technique is best suited w.r.t. accuracy and task completion time by pairwise comparison.
3. Finally, we provide a descriptive analysis.

**6.2.1. Statistical Analysis Regarding the Accuracy**

**First Stage.** The first analysis stage determines whether there is significant difference between the three visualization techniques w.r.t. the amount of right answers, recall Tab. 4. Box plots for the accuracy for  $Vis_A$ ,  $Vis_B$  and  $Vis_C$  are provided in Figure 8. Initially, we employ the *Shapiro-Wilk* test separately for  $Vis_A$ ,  $Vis_B$  and  $Vis_C$  to determine whether the amount of right answers is normally distributed. Hence, the null-hypothesis  $H_0$  of the test states a normal distribution of the random variable:

$$H_0 : \text{The random variable is normally distributed.}$$

The Shapiro-Wilk test yields the following significance levels:

- 0.003 for  $Vis_A$ , and
- 0.037 for  $Vis_B$ , and
- 0.000 for  $Vis_C$ .

Since  $H_0$  is rejected, if the significance level is smaller than 0.05, the accuracy significantly deviates from a normal distribution for each visualization technique. The next step comprises the analysis, whether the visualization techniques are significantly different. We chose the *Friedmann test*, since this test provides an ANOVA for random variables that are not normally distributed. We define the hypothesis:

$H_0$  : All visualization techniques achieve similar results.

Advantageously, the *Friedmann test* is based on ranks and not the actual scores. The *Friedman test* reveals that the accuracies significantly differ for the three visualizations, with  $\chi^2(2) = 25.382$ ,  $p < .05$ , and the hypothesis  $H_0$  must be rejected.

**Second Stage.** In the second analysis stage, we compare the visualization techniques to identify the best one w.r.t. accuracy. Based on the previous results, i.e., the amounts of right answers are not normally distributed and are significantly different, we carry out a pair-wise comparison of the visualizations. Since we deal with non-parametric data, we apply the *Wilcoxon signed-rank test* for  $Vis_A$ ,  $Vis_B$  and  $Vis_C$ . A correction with the *Bonferroni procedure* [Sha95] was applied, since we carry out multiple tests on the participants' responses. Thus, all effects are reported at a .0167 level of significance, i.e., a third of 0.05. The amount of correct answers were significantly higher for  $Vis_A$  ( $m = 4.5$ ) than for  $Vis_B$  ( $m = 3.0$ ),  $U = -3.76$ ,  $p < .0167$ , where  $m$  denotes the median. Also, the amount of correct answers was significantly higher for  $Vis_C$  ( $m = 5.0$ ) than for  $Vis_B$  ( $m = 3.0$ ),  $U = -4.07$ ,  $p < .0167$ . However, there was no significant difference between  $Vis_A$  ( $m = 4.5$ ) and  $Vis_C$  ( $m = 5.0$ ),  $U = 0.95$ ,  $p = .354$ . The resulting box plots for  $Vis_A$ ,  $Vis_B$  and  $Vis_C$  are provided in Figure 8.

Since  $Vis_B$  significantly differs from  $Vis_A$  and  $Vis_C$ , we analyzed how it competes with guessing, where guessing would result in three correct answers. Hence, a *Wilcoxon signed rank test* yields a significant difference ( $U = -2,094$ ,  $p < .05$  with  $\mu_{Vis_B} < \mu_{guessing}$ ). Thus,  $Vis_B$  may systematically influence the users to provide wrong answers.

**Third Stage.** When using  $Vis_C$  ( $\mu = 4.47$ ,  $\sigma = 1.16$ ) and  $Vis_A$  ( $\mu = 4.06$ ,  $\sigma = 1.67$ ), the participants achieved a higher accuracy than

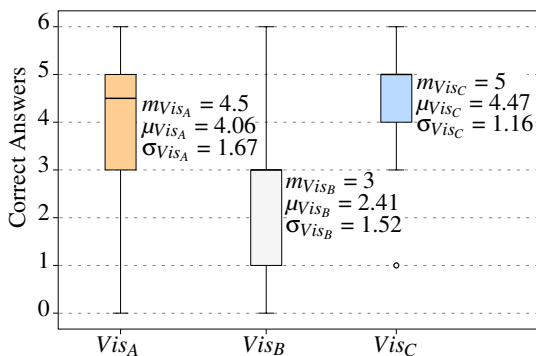


**Figure 8:** Box plots of the accuracy for  $Vis_A$ ,  $Vis_B$  and  $Vis_C$  including the median  $m$ , the mean  $\mu$  and the standard deviation  $\sigma$ .

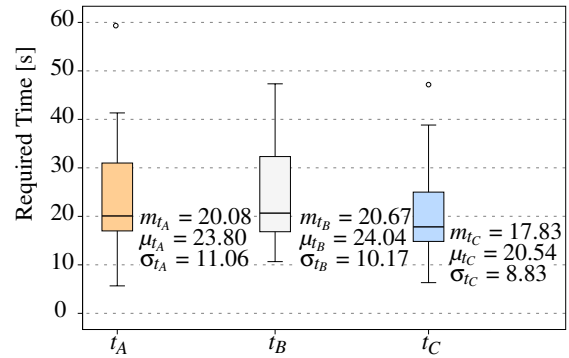


**Figure 9:** Box plots of the averaged task completion times  $t_A$ ,  $t_B$ , and  $t_C$  including the median  $m$ , the mean  $\mu$  and the standard deviation  $\sigma$ .

with  $Vis_B$  ( $\mu = 2.41$ ,  $\sigma = 1.52$ ). Comparison of the mean values of  $Vis_A$  and  $Vis_C$  indicates the superiority of  $Vis_C$ .

## 6.2.2. Statistical Analysis Regarding the Required Time

For each visualization technique, the task completion time was logged. We averaged the task completion time for each question, i.e., we extract the average time  $t_A$ ,  $t_B$  and  $t_C$  required by the users for a single question using  $Vis_A$ ,  $Vis_B$ , or  $Vis_C$ , respectively (recall Tab. 4). The boxplots are depicted in Figure 9. Similar to the previous analysis, we first determine whether there is a statistically significant difference between  $t_A$ ,  $t_B$  and  $t_C$ . We employ the *Shapiro-Wilk test* to determine whether the required times are normally distributed yielding the following significance levels:

- 0.029 for  $t_A$ , and
- 0.007 for  $t_B$ , and
- 0.006 for  $t_C$ .

Hence, all three variables significantly deviate from a normal distribution ( $p < 0.05$ ).

As proposed for statistical analysis of  $Vis_A$ ,  $Vis_B$  and  $Vis_C$  w.r.t. the accuracy, the second stage determines whether  $t_A$ ,  $t_B$  and  $t_C$  are significantly different. Therefore, we carry out the *Friedmann test*, since this test provides an ANOVA for random variables that are not normally distributed. The corresponding null-hypothesis is:

$H_0$  : The task completion time differs for  $Vis_A$ ,  $Vis_B$  and  $Vis_C$ .

As a result, the *Friedman test* reveals no significant difference, i.e.,  $\chi^2(2) = 2.8$ , and  $p > 0.05$ . Thus,  $H_0$  cannot be rejected.

**Second Stage.** Since no statistically significant difference could be shown by the *Friedmann test*, we do not carry out a pairwise comparison of the task completion times.

**Third Stage.** Comparing the box plots and test statistics of  $t_A$ ,  $t_B$  and  $t_C$ , the participants performed the tasks in average faster with  $Vis_C$  ( $\mu = 20.54$ ,  $\sigma = 8.83$ ) compared to  $Vis_A$  ( $\mu = 23.80$ ,  $\sigma = 11.06$ ) and  $Vis_B$  ( $\mu = 24.04$ ,  $\sigma = 10.17$ ). Comparing the mean values of  $t_A$  and  $t_B$ , the users required more time to fulfill the tasks with  $Vis_B$ .



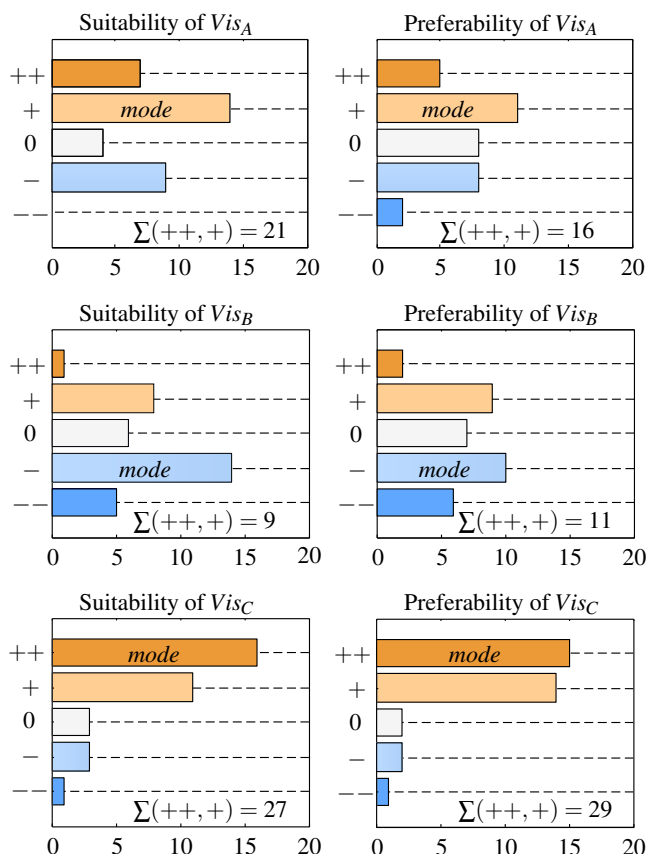


**Figure 10:** Evaluation results of the participants regarding suitability and preferability of  $Vis_A$ ,  $Vis_B$ , and  $Vis_C$ . The mode value, i.e., the answer that was given most often for each question, is marked. Furthermore, the sum of answers ++ and + is provided.

### 6.2.3. Qualitative Evaluation of Suitability and Preferability

When analyzing the suitability and preferability ratings, the same trends are reflected, see Figure 10. Furthermore, the mode value, i.e., the answer (–, –, 0, +, ++) that was given most often for each question, as well as the amount of users that provide answer ++ and + is provided. Hence, users mostly rated  $Vis_C$  with ++ for suitability as well as preferability,  $Vis_A$  with + for suitability as well as preferability and  $Vis_B$  with – for suitability as well as preferability. The amount of users rating  $Vis_C$  as suitable and very suitable (i.e., answers are + or ++) was highest with 27, followed by 21 for  $Vis_A$  and 9 for  $Vis_B$ . Similarly, the amount of users rating  $Vis_C$  as preferable and very preferable (i.e., answers are + or ++) was highest with 29, followed by 16 for  $Vis_A$  and 11 for  $Vis_B$ .

## 7. Discussion

The statistical analysis revealed a significant difference of  $Vis_A$ ,  $Vis_B$  and  $Vis_C$  w.r.t. accuracy. The pair-wise comparison identifies  $Vis_B$  as poorest choice. It does not only achieve lower mean values compared to  $Vis_A$  and  $Vis_C$ , but significantly differs from both as well.  $Vis_C$  is not statistically significant different from  $Vis_A$ , how-

ever, due to the higher mean values compared to  $Vis_A$ , it is declared as the best visualization to compare the volume of two aneurysms. A possible conclusion might be that a derived quantity, i.e., the distance, improves the identification of the larger aneurysm. Furthermore, mean and median values of  $t_C$  were smaller than the values of  $t_A$  and  $t_B$ . Although no significant difference occurred, these test results rate  $Vis_C$  as best visualization w.r.t. task completion time.

Remarkably,  $Vis_B$  even achieved a lower success rate than guessing. This is interpreted as indication that the users did not fully understand the design of  $Vis_B$  and that  $Vis_B$  is very inappropriate for comparison of surfaces. We assume that users wrongly interpret the ghosting view and thus, do not focus on the border areas but instead on areas with surface normals parallel to the current viewing direction. These areas are pre-dominantly color-coded in cyan, since the  $A_{Comp}$  aneurysm is always drawn after the orange  $A_{Ref}$  aneurysm.

When analyzing the suitability and preferability ratings, we found overwhelming preference for  $Vis_A$  and  $Vis_C$  over  $Vis_B$  which further indicates the inappropriateness of the latter. There was also a small trend towards preferring  $Vis_C$  over  $Vis_A$ , identifying  $Vis_C$  as favorite visualization.

## 8. Conclusion

Researchers involved in medical applications are often confronted with visualization techniques, which are rather difficult to evaluate. Many times, medical visualization papers lack a quantitative evaluation at all. With our proposed user study, a pipeline was presented, which allows the comparative evaluation for three different visualization techniques for the specific application of cerebral aneurysm volume assessment. With focus on accuracy and task completion time, this concept can be easily applied to various scenarios to support qualitative findings with quantitative results.

For the evaluation of the aneurysm volume, the visualization should be reduced to basic information, i.e., no ghosted view techniques should be employed. Providing a color-coded surface visualization with quantitative distance information such as our new visualization technique  $Vis_C$ , helps the users to decide which aneurysm exhibits the largest volume. This was reflected by a statistically significant higher accuracy, a smaller task completion time as well as a better user rating.

For future work, different approaches can be pursued. The visualizations can be improved, for example by including depth cues such as ambient occlusion. From the statistical point of view, a systematic analysis of the influence of the volume change could be carried out. Hence, a visualization technique may be well-suited for the depiction of large volume changes, but rather improperly suited for small volume changes with a second visualization technique exhibiting the opposite behavior. Finally, we chose the employed colors to prevent false interpretations due to red-green color blindness. In future, different color blindness types should be considered and assessed with the questionnaire.

**Acknowledgements** We warmly thank Alexandra Baer and Maria Luz for fruitful discussions and guidance for the evaluation. We also thank the Institute for Neuroradiology, University of Magdeburg, for providing the medical image data. This work

was partially funded by the Federal Ministry of Education and Research within the Forschungscampus *STIMULATE* (grant number ‘13GW0095A’).

## References

- [BBF\*11] BUSKING S., BOTHA C. P., FERRARINI L., MILLES J., POST F. H.: Image-based rendering of intersecting surfaces for dynamic comparative visualization. *The Visual Computer* 27, 5 (2011), 347–363. 2
- [BCFW08] BARTZ D., CUNNINGHAM D., FISCHER J., WALLRAVEN C.: The role of perception for computer graphics. *Eurographics state-of-the-art-reports* (2008), 65–86. 2
- [BFLC04] BÜHLER K., FELKEL P., LA CRUZ A.: *Geometric methods for vessel visualization and quantification—a survey*. Springer, 2004. 2
- [BGCP11] BAER A., GASTEIGER R., CUNNINGHAM D., PREIM B.: Perceptual evaluation of ghosted view techniques for the exploration of vascular structures and embedded flow. *Computer Graphics Forum* 30, 3 (2011), 811–820. 2
- [BGP\*11] BORKIN M., GAJOS K., PETERS A., MITSOURAS D., MELCHIONNA S., RYBICKI F., FELDMAN C., PFISTER H.: Evaluation of artery visualizations for heart disease diagnosis. *IEEE Transactions on Visualization and Computer Graphics* 17, 12 (2011), 2479–2488. 2
- [BRB\*15] BERG P., ROLOFF C., BEUING O., VOSS S., SUGIYAMA S., ARISTOKLEOUS N., ET AL.: The Computational Fluid Dynamics Rupture Challenge 2013 – Phase II: variability of hemodynamic simulations in two intracranial aneurysms. *Journal of Biomechanical Engineering* 137, 12 (2015), 121008/1–13. 1
- [CCA\*05] CEBRAL J. R., CASTRO M. A., APPANABOYINA S., PUTMAN C. M., MILLAN D., FRANGI A. F.: Efficient pipeline for image-based patient-specific analysis of cerebral aneurysm hemodynamics: technique and sensitivity. *IEEE Transactions on Medical Imaging* 24, 4 (2005), 457–467. 1, 3
- [CFM\*13] CARNECKY R., FUCHS R., MEHL S., JANG Y., PEIKERT R.: Smart transparency for illustrative visualization of complex flow surfaces. *IEEE Transactions on Visualization and Computer Graphics* 19, 5 (2013), 838–851. 2
- [CSP10] CEBRAL J. R., SHERIDAN M., PUTMAN C. M.: Hemodynamics and bleb formation in intracranial aneurysms. *American Journal of Neuroradiology*, 31, 2 (2010), 304–310. 2
- [DRN\*15] DÍAZ J., ROPINSKI T., NAVAZO I., GOBBETTI E., VÁZQUEZ P.-P.: An experimental study on the effects of shading in 3d perception of volumetric models. *The Visual Computer* (2015), 1–15. 2
- [GBNP15] GLASSER S., BERG P., NEUGEBAUER M., PREIM B.: Reconstruction of 3d surface meshes for blood flow simulations of intracranial aneurysms. In *Proc. of Computer and Robotic Assisted Surgery (CURAC)* (2015), pp. 163–168. 1
- [GLH\*14] GLASSER S., LAWONN K., HOFFMANN T., SKALEJ M., PREIM B.: Combined visualization of wall thickness and wall shear stress for the evaluation of aneurysms. *IEEE Transactions on Visualization and Computer Graphics (TVCG)* (2014), 2506–2515. 4
- [GLR\*09] GEERS A. J., LARRABIDE I., RADAELLI A., BOGUNOVIC H., VAN ANDEL H., MAJOIE C., FRANGI A. F.: Reproducibility of image-based computational hemodynamics in intracranial aneurysms: comparison of CTA and 3DRA. In *Proc. of IEEE Symposium on Biomedical Imaging: From Nano to Macro (ISBI)* (2009), pp. 610–613. 3
- [GNKP10] GASTEIGER R., NEUGEBAUER M., KUBISCH C., PREIM B.: Visualization of cerebral aneurysms with embedded blood flow information. In *Proc. of the Eurographics Workshop on Visual Computing for Biology and Medicine (VCBM)* (2010), pp. 25–32. 2, 4
- [GR04] GRIGORYAN G., RHEINGANS P.: Point-based probabilistic surfaces to show surface uncertainty. *IEEE Transactions on Visualization and Computer Graphics* 10, 5 (2004), 564–573. 2
- [GSK\*15] GEURTS A., SAKAS G., KUIJPER A., BECKER M., VON LANDESBERGER T.: Visual comparison of 3d medical image segmentation algorithms based on statistical shape models. In *Digital Human Modeling. Applications in Health, Safety, Ergonomics and Risk Management: Ergonomics and Health*. Springer, 2015, pp. 336–344. 2
- [IIC\*13] ISENBERG T., ISENBERG P., CHEN J., SEDLMAIR M., MOLLER T.: A systematic review on the practice of evaluating visualization. *IEEE Transactions on Visualization and Computer Graphics* 19, 12 (2013), 2818–2827. 2
- [KHI\*03] KOSARA R., HEALEY C. G., INTERRANTE V., LAIDLAW D. H., WARE C.: User studies: why, how, and when? *IEEE Computer Graphics and Applications* 23, 4 (2003), 20–25. 2
- [LABFL09] LESAGE D., ANGELINI E. D., BLOCH I., FUNKA-LEA G.: A review of 3D vessel lumen segmentation techniques: models, features and extraction schemes. *Medical Image Analysis* 13, 6 (2009), 819–845. 1
- [LEBB09] LALL R. R., EDDLEMAN C. S., BENDOK B. R., BATJER H. H.: Unruptured intracranial aneurysms and the assessment of rupture risk based on anatomical and morphological factors: sifting through the sands of data. *Neurosurgical Focus* 26, 5 (2009), E2. 1, 2
- [MMG15] MIAO H., MISTELBAUER G., NAŠEL C., GRÖLLER M. E.: Cowrader: Visual quantification of the circle of willis in stroke patients. In *Proc. of the Eurographics Workshop on Visual Computing for Biology and Medicine (VCBM)* (2015), pp. 1–10. 2
- [NLBP13] NEUGEBAUER M., LAWONN K., BEUING O., PREIM B.: Automatic generation of anatomic characteristics from cerebral aneurysm surface models. *International Journal of Computer Assisted Radiology and Surgery* 8, 2 (2013), 279–289. 3
- [PBC\*16] PREIM B., BAER A., CUNNINGHAM D., ISENBERG T., ROPINSKI T.: A survey of perceptually motivated 3d visualization of medical image data. *Computer Graphics Forum* 35, 3 (2016), 501–525. 2
- [PH11] PÖTHKOW K., HEGE H.-C.: Positional uncertainty of isocontours: Condition analysis and probabilistic measures. *IEEE Transactions on Visualization and Computer Graphics* 17, 10 (2011), 1393–1406. 2
- [PO08] PREIM B., OELTZE S.: 3d visualization of vasculature: an overview. In *Visualization in medicine and life sciences*. Springer, 2008, pp. 39–59. 2
- [PRJ12] POTTER K., ROSEN P., JOHNSON C. R.: From quantification to visualization: a taxonomy of uncertainty visualization approaches. In *Uncertainty Quantification in Scientific Computing*, Dienstfrey A., Boisvert R., (Eds.), vol. 377. Springer, 2012, pp. 226–249. 2
- [Sha95] SHAFFER J. P.: Multiple hypothesis testing. *Annual Review of Psychology* 46 (1995), 561–584. 8
- [SOBP07] SCHUMANN C., OELTZE S., BADE R., PREIM B.: Model-free surface visualization of vascular trees. In *Proc. of IEEE/Eurographics Symposium on Visualization (EuroVis)* (2007), pp. 283–290. 2
- [Wie03] WIEBERS D. O.: Unruptured intracranial aneurysms: natural history, clinical outcome, and risks of surgical and endovascular treatment. *The Lancet*, 9378 (2003), 103–110. 2
- [WT05] WEIGLE C., TAYLOR R. M.: Visualizing intersecting surfaces with nested-surface techniques. In *Proc. of IEEE Visualization* (2005), pp. 503–510. 2
- [WvdSAR07] WERMER M. J., VAN DER SCHAAF I. C., ALGRA A., RINKE G. J.: Risk of rupture of unruptured intracranial aneurysms in relation to patient and aneurysm characteristics: an updated meta-analysis. *Stroke* 38, 4 (2007), 1404–1410. 2
- [XNT\*11] XIANG J., NATARAJAN S. K., TREMMEL M., MA D., MOCCO J., HOPKINS L. N., SIDDIQUI A. H., LEVY E. I., MENG H.: Hemodynamic-morphologic discriminants for intracranial aneurysm rupture. *Stroke* 42, 1 (2011), 144–152. 3